AIAA JOURNAL
Vol. 33, No. 12, December 1995

Unified Turbulence Closure Model for Axisymmetric and Planar Free Shear Flows

David F. Robinson*
North Carolina State University, Raleigh, North Carolina 27695-7910
Julius E. Harris†
NASA Langley Research Center, Hampton, Virginia 23681-0001
and
H. A. Hassan‡
North Carolina State University, Raleigh, North Carolina 27695-7910

A new two-equation turbulence model based on the exact turbulent kinetic energy and the variance of vorticity or enstrophy equations is developed and used to calculate planar and axisymmetric free shear flows. It is shown that one set of model constants reproduces available growth rates and similarity profiles of velocity and shear stress. In general, agreement is well within the scatter of experimental data.

Introduction

EXISTING two-equation turbulence models require different model constants and different boundary conditions for the successful prediction of growth rates of wakes, jets, and mixing layers.[1] Moreover, attempts at using turbulent stress models have failed to improve agreement between theory and experiment for such flows.[2] Development of a unified closure model that is capable of describing these flows using the same set of model constants and the same boundary conditions would represent a major step toward the development of a three-dimensional model for both bounded and free shear flows.

After an exhaustive study of free shear flows, Morse[2] concluded that the primary cause for failure of existing turbulence models is the inadequate modeling of the equation for the dissipation rate. It is safe to assume that for large turbulence Reynolds numbers the small scales are independent of the large scales and the mean flow. Thus, their rate of dissipation is isotropic. This assumption forms the basis of almost all ε or ω equations. If, on the other hand, the turbulent Reynolds stress is not large, the dissipation rate will be slightly anisotropic and terms that appear in the exact dissipation equation that depend on the mean flow, although small, may not be negligible. Based on this argument, Morse developed equations for the nonisotropic dissipation tensor ε_{ij}. Unfortunately, the form of the equations used to describe ε_{ij} did not help resolve the round jet anomaly.

Our objective in this work is to resolve all anomalies associated with free shear flows and, in the process, chart a new approach for modeling wall bounded and free shear flows. Morse concluded that the eddy viscosity assumption was not the cause of the round jet anomaly. Therefore, the approach to be presented here will be based on a two-equation model. Extension to a stress model will be discussed separately. Rather than develop equations for the dissipation rate tensor as was done by Morse, our approach will be based on the exact dissipation equation. Thus, terms that depend on the mean flow that are negligible at high turbulent Reynolds numbers but not at low turbulent Reynolds numbers will be retained and modeled.

Instead of using the exact dissipation equation, we opted to use the exact equation governing the vorticity variance, or enstrophy.[3] The two equations are equivalent. This was done for two reasons. First, vortex stretching plays a major role in the production of turbulence. Thus, a modeled equation governing a property of the fluctuating vorticity should be more descriptive of the physics of turbulence. The second is that the (incompressible) enstrophy equation has no explicit dependence on the pressure. Because all free shear flows considered in this work have constant pressure, the significance of this choice will become clear when the current approach is applied to wall bounded shear flows in the presence of strong pressure gradients.

The enstrophy equation has a number of well-defined terms describing various sources of production (destruction).[3] Thus, in addition to the gradient production term, there is production by vortex stretching and the mean strain rate. Rather than combine all of these terms together, almost all of the terms were modeled separately.

The enstrophy equation has been the subject of detailed investigation by Bernard and Berger,[4] Raul and Bernard,[5] Bernard,[6] and Gorski.[7] They utilized Lagrangian time expansion techniques to effect closure. The early work resulted in equations that were not suited for immediate inclusion in available computational fluid dynamics (CFD) codes. As a result, the work did not receive the wide attention it deserves. This, however, was remedied by Gorski.[7] Our approach in modeling the enstrophy equation is given subsequently and is quite different from that of Refs. 4–7. The resulting equation can be easily incorporated into existing CFD codes by substituting the enstrophy equation for the ε or ω equation.

Because of the increased number of terms in the enstrophy equation, the number of model constants is increased. These were evaluated by requiring the modeling to be consistent with the scaling in the log-law region and by numerical optimization. The latter entailed the requirement that the model give the best prediction of growth rate, velocity, and shear stress distribution in the similarity region for the round jet. Thus, no attempt was made to utilize results of the decay of homogeneous turbulence in selecting the model constants. The resulting set of constants were then used to calculate plane wakes, plane and radial jets, mixing layers, and homogeneous shear flows. The results are compared with available experiment. In general, agreement is well within experimental scatter.

Formulation of the Problem

Governing Equations

Assuming incompressible flow, the governing equations are the

Received Oct. 31, 1994; presented as Paper 95-0360 at the AIAA 33rd Aerospace Sciences Meeting, Reno, NV, Jan. 9–12, 1995; revision received April 18, 1995; accepted for publication June 23, 1995.

*Research Assistant, Mechanical and Aerospace Engineering. Student Member AIAA.
†Senior Research Scientist, Flow Modeling and Control Branch. Associate Fellow AIAA.
‡Professor, Mechanical and Aerospace Engineering. Associate Fellow AIAA.

Reynolds averaged continuity, momentum, turbulent kinetic energy, and enstrophy. These equations can be written as

$$\frac{\partial U_i}{\partial x_i} = 0 \tag{1}$$

$$\rho \frac{\mathrm{D}U_i}{\mathrm{D}t} = -\frac{\partial P}{\partial x_i} + \frac{\partial}{\partial x_i}(2\mu S_{ij} - \overline{\rho u_i' u_j'}) \tag{2}$$

$$\rho \frac{\mathrm{D}k}{\mathrm{D}t} = \tau_{im}\frac{\partial U_i}{\partial x_m} - \mu\overline{\frac{\partial u_i'}{\partial x_m}\frac{\partial u_i'}{\partial x_m}} - \frac{\partial}{\partial x_m}\left[\rho\frac{\overline{u_i' u_i' u_m'}}{2} + \overline{p' u_m'} - \mu\frac{\partial k}{\partial x_m}\right] = \tau_{im}\frac{\partial U_i}{\partial x_m} - \mu\zeta - \frac{\partial}{\partial x_m}\left[\frac{\overline{\rho u_i' u_i' u_m'}}{2} + \overline{p' u_m'} - \mu\varepsilon_{ikm}\frac{\partial(\overline{u_i'\omega_m'})}{\partial x_k}\right] \tag{3}$$

$$\frac{\mathrm{D}\zeta}{\mathrm{D}t} = -2\overline{u_j'\omega_i'}\frac{\partial\Omega_i}{\partial x_j} - \frac{\partial(\overline{u_j'\omega_i'\omega_i'})}{\partial x_j} + 2\overline{\omega_j'\omega_j' s_{ij}'} + 2\overline{\omega_i'\omega_j'}S_{ij} + 2\overline{\omega_i' s_{ij}'}\Omega_j + \nu\frac{\partial^2\zeta}{\partial x_j\partial x_j} - 2\nu\overline{\frac{\partial\omega_j'}{\partial x_j}\frac{\partial\omega_i'}{\partial x_j}} \tag{4}$$

where

$$s_{ij}' = \frac{1}{2}\left(\frac{\partial u_i'}{\partial x_j} + \frac{\partial u_j'}{\partial x_i}\right) \qquad S_{ij} = \frac{1}{2}\left(\frac{\partial U_i}{\partial x_j} + \frac{\partial U_j}{\partial x_i}\right)$$
$$\Omega_i = \varepsilon_{ijk}\frac{\partial U_k}{\partial x_j} \qquad \omega_i' = \varepsilon_{ijk}\frac{\partial u_k'}{\partial x_j} \tag{5}$$
$$k = \overline{u_i' u_i'}/2 \qquad \zeta = \overline{\omega_i'\omega_i'}$$
$$\tau_{ij} = -\overline{\rho u_i' u_j'} \qquad \nu = \mu/\rho$$

where ρ is the density, μ is the viscosity, u_i', ω_i', and p' are the fluctuating velocity, vorticity, and pressure, U_i is the mean velocity, and ε_{ijk} is the permutation tensor.

Modeling of the Enstrophy Equation

Using the Boussinesq assumption, the turbulent stress tensor can be written as

$$\tau_{ij} = 2\rho[\nu_t S_{ij} - (k/3)\delta_{ij}] \tag{6}$$

where δ_{ij} is the Kronecker delta and ν_t is the eddy viscosity. There are six terms that require modeling in the enstrophy equation. The following guidelines were followed in obtaining the modeled equation: dimensional consistency, coordinate system independence, Galilean invariance, linear relationships, and the least number of possible model constants. As will be seen, we will encounter symmetric and skew-symmetric tensors that require modeling. The symmetric tensors are expressed in terms of τ_{ij}, S_{ij}, and δ_{ij}, whereas the skew-symmetric tensors are expressed in terms of Ω_{ij}, the rotation tensor, and

$$\frac{\partial k}{\partial x_i}\frac{\partial\zeta}{\partial x_j} - \frac{\partial k}{\partial x_j}\frac{\partial\zeta}{\partial x_i}$$

The quantity $\overline{\omega_i' u_j'}$ is a second-order tensor. It can be written as the sum of symmetric and skew-symmetric tensors, i.e.,

$$\overline{\omega_i' u_j'} = \tfrac{1}{2}(\overline{\omega_i' u_j' + \omega_j' u_i'}) + \tfrac{1}{2}(\overline{\omega_i' u_j' - \omega_j' u_i'}) = A_{ij} + B_{ij} \tag{7}$$

From the identity

$$\varepsilon_{mij}\overline{\omega_i' u_j'} = \frac{\partial(\overline{u_m' u_i'})}{\partial x_i} - \frac{\partial k}{\partial x_m} \tag{8}$$

one finds

$$B_{ij} = \frac{\varepsilon_{mij}}{2}\left[\frac{\partial(\overline{u_m' u_\ell'})}{\partial x_\ell} - \frac{\partial k}{\partial x_m}\right] \tag{9}$$

The symmetric part is modeled as follows. From

$$\overline{\omega_i' u_j'} = \varepsilon_{im\ell}\overline{\frac{\partial u_\ell'}{\partial x_m}u_j'} = \varepsilon_{im\ell}\overline{u_j' r_{\ell m}'} \tag{10}$$

where

$$r_{\ell m}' = \frac{1}{2}\left(\frac{\partial u_\ell'}{\partial x_m} - \frac{\partial u_m'}{\partial x_\ell}\right) \tag{11}$$

The term $\overline{u_j' r_{\ell m}'}$ is modeled using a gradient diffusion assumption

$$\overline{u_j' r_{\ell m}'} = \frac{\nu_t}{\sigma_R}\frac{\partial\Omega_{\ell m}}{\partial x_j} \tag{12}$$

Using Eqs. (7), (9), (10), and (12) one finds

$$\overline{u_j'\omega_i'} = \frac{\nu_t}{2\sigma_R}\left[\frac{\partial\Omega_i}{\partial x_j} + \frac{\partial\Omega_j}{\partial x_i}\right] + \frac{\varepsilon_{mij}}{2}\left[\frac{\partial(\overline{u_m' u_\ell'})}{\partial x_\ell} - \frac{\partial k}{\partial x_m}\right] \tag{13}$$

where σ_R is a model constant.

Using the gradient diffusion assumption, the term $(\partial/\partial x_j)(\overline{u_j'\omega_i'\omega_i'})$ can be written as

$$\frac{\partial(\overline{u_j'\omega_i'\omega_i'})}{\partial x_j} = -\frac{\partial}{\partial x_j}\left[\frac{\nu_t}{\sigma_\zeta}\frac{\partial\zeta}{\partial x_j}\right] \tag{14}$$

where σ_ζ is a model constant.

For the quantity $\omega_i'\omega_j' s_{ij}' - \nu(\partial\omega_i'/\partial x_j)(\partial\omega_i'/\partial x_j)$, the first term represents vortex stretching and the second represents dissipation. Both Tennekes and Lumley[3] and Reynolds[8] show that the two terms are large but comparable at high turbulent Reynolds numbers. Because of this, Reynolds[8] and Bernard and Speziale[9] suggested that the two terms be modeled together. For high turbulent Reynolds numbers, the term is modeled as

$$R_k(A - B)\nu\zeta^2/k, \qquad R_k = \sqrt{R_t}, \qquad R_t = k^2/\nu^2\zeta \tag{15}$$

with

$$A = \frac{7}{3\sqrt{15}}S_k(0), \qquad B = \frac{7}{3\sqrt{15}}G_k + \frac{\beta_5}{R_k} \tag{16}$$

and $S_k(0)$, G_k, and β_5 are model constants. Reynolds assumes $S_k(0) = G_k$, whereas Bernard and Speziale assume $S_k(0) \neq G_k$ with the difference, however, being small. Because of this, the Reynolds assumption is employed here. To allow for the effects of anisotropy at lower turbulent Reynolds numbers, an additional term

$$\beta_7\zeta\frac{\Omega_i\Omega_j}{\Omega^2}S_{ij}; \qquad \Omega^2 = \Omega_i\Omega_i \tag{17}$$

was added with β_7 being a model constant. As a result,

$$\overline{\omega_i'\omega_j' s_{ij}'} - \nu\overline{\frac{\partial\omega_i'}{\partial x_j}\frac{\partial\omega_i'}{\partial x_j}} = \frac{\beta_7\zeta}{\Omega^2}\Omega_i\Omega_j S_{ij} - \frac{\beta_5\zeta^{\frac{3}{2}}}{\sqrt{R_t}} \tag{18}$$

The term shown in Eq. (17) is zero for two-dimensional flows. Therefore, it is similar in spirit to a term introduced by Pope[10] in his attempt to resolve the round jet anomaly. Unfortunately, as was pointed out by Rubel,[11] introduction of Pope's term resulted in a radial jet anomaly. Because of this, Pope's correction was never adopted.

The term $\overline{\omega_i'\omega_j'}$ is modeled as

$$\overline{\omega_i\omega_j} = \alpha_3\zeta b_{ij} + \tfrac{2}{3}\delta_{ij}\zeta \tag{19}$$

where

$$b_{ij} = \left[\frac{-\overline{u_i' u_j'}}{k} + \frac{2}{3}\delta_{ij}\right] \tag{20}$$

and α_3 is a model constant.

The term $\overline{\omega_i' s_{ij}'}$ is a vector and can be modeled as

$$\overline{\omega_i' s_{ij}'} = C_1 \tau_{ij}\Omega_i + C_2 \tau_{ij}\varepsilon_{i\ell m}\left(\frac{\partial k}{\partial x_m}\frac{\partial \zeta}{\partial x_\ell} - \frac{\partial k}{\partial x_\ell}\frac{\partial \zeta}{\partial x_m}\right) \tag{21}$$

with C_1 and C_2 determined from dimensional considerations as

$$C_1 = -\frac{1}{\rho k}\left[\beta_4 \frac{\zeta}{\Omega} + \beta_6 \frac{\nu_t}{\nu}\Omega\right], \qquad C_2 = \frac{\beta_8}{\rho k \Omega^2} \tag{22}$$

where β_4, β_6, and β_8 are model constants. Combining the various terms, the modeled enstrophy equation takes the form

$$\begin{aligned}\frac{\mathrm{D}\zeta}{\mathrm{D}t} &= -\frac{\partial \Omega_i}{\partial x_j}\left(\frac{\nu_t}{\sigma_r}\left[\frac{\partial \Omega_i}{\partial x_j} + \frac{\partial \Omega_j}{\partial x_i}\right]\right) \\ &- \varepsilon_{mij}\frac{\partial \Omega_i}{\partial x j}\left[\frac{\partial(\overline{u_m' u_\ell'})}{\partial x_\ell} - \frac{\partial k}{\partial x_m}\right] + \frac{\partial}{\partial x_j}\left[\left(\nu + \frac{\nu_t}{\sigma_\zeta}\right)\frac{\partial \zeta}{\partial x_j}\right] \\ &- \frac{\beta_5}{R_k}\zeta^{\frac{3}{2}} + \left(\alpha_3 \zeta b_{ij} + \frac{2}{3}\delta_{ij}\zeta\right)S_{ij} - \frac{\beta_4 \zeta \tau_{ij}\Omega_i\Omega_j}{\rho k \Omega} \\ &+ \varepsilon_{i\ell m}\beta_8\left(\frac{\tau_{ij}}{\rho k}\right)\left(\frac{\partial k}{\partial x_\ell}\frac{\partial \zeta}{\partial x_m} - \frac{\partial k}{\partial x_m}\frac{\partial \zeta}{\partial x_\ell}\right)\frac{\Omega_j}{\Omega^2} \\ &- 2\frac{\beta_6 \tau_{ij}\nu_t}{\rho k \nu}\Omega\Omega_i\Omega_j + \frac{\beta_7 \zeta}{\Omega^2}\Omega_i\Omega_j S_{ij}\end{aligned} \tag{23}$$

with

$$R_k = k/\nu\sqrt{\zeta} \tag{24}$$

Using Eq. (13), the modeled turbulent kinetic energy equation can be expressed as

$$\rho\frac{\mathrm{D}k}{\mathrm{D}t} = \tau_{im}\frac{\partial U_i}{\partial x_m} - \mu\zeta + \frac{\partial}{\partial x_m}\left[\left(\frac{\mu}{3} + \frac{\mu_t}{\sigma_k}\right)\frac{\partial k}{\partial x_m}\right] \tag{25}$$

where σ_k is a model constant.

Model Constants

The first requirement in determining model constants is to comply with the scaling in the log-law region. In the log-law region

$$u^+ = (1/\kappa)\ell n y^+ + B \tag{26}$$

where

$$u^+ = u/u_\tau, \quad y^+ = y u_\tau/\nu, \quad u_\tau = \sqrt{\tau_\omega/\rho} \tag{27}$$

where τ_ω is the wall shearing stress and κ is the Kármán constant. From the requirement that

$$\tau = \tau_\omega, \qquad -(\overline{u'v'}/k) = \sqrt{C_\mu} \tag{28}$$

we obtain

$$k = u_\tau^2/\sqrt{C_\mu}, \qquad \zeta = u_\tau^3/\nu k y, \qquad \nu_t = \kappa u_\tau y \tag{29}$$

Substituting Eq. (29) into Eq. (23) yields

$$\sigma_r = \frac{1}{2}, \qquad \sigma_\zeta = \frac{6\kappa^2}{6\beta_5\sqrt{C_\mu} - 3\alpha_3\sqrt{C_\mu} - 4\beta_4 - 8\beta_6} \tag{30}$$

The remaining coefficients may be obtained by numerical optimization. Advantage is taken of the fact that at some distance downstream of a generating body, the flow reaches a self-similar or a self-preserving state. The resulting total differential equations can be solved and compared with available experimental data. There is an abundance of turbulent measurements for free shear flows. It should be noted, however, that there is a lack of consistency amongst various experiments involving normal stresses and turbulent kinetic energy. Therefore, model constants were optimized by emphasizing comparisons with measured growth rates and similarity profiles of velocity and shear stress.

Table 1 Turbulence model closure coefficients constants

Constants	k–ζ
C_μ	0.09
κ	0.40
α_3	0.35
β_4	0.42
β_5	2.37
β_6	0.10
β_7	0.75
β_8	2.30
$1/\sigma_k$	1.80
$1/\sigma_\zeta$	1.46

The plan then was to choose one of the free shear flows, such as the round jet, and optimize the model coefficients. After this was accomplished, the governing equations were then used to calculate the other results presented in the paper.

The resulting self-similar equations are plagued with a numerical singularity associated with the edge of the shear layer. For fully turbulent flows, the edge of a shear layer corresponds to a sharp turbulent–nonturbulent interface. Paullay et al.[12] introduced a transformation that moved the finite edge to infinity. This transformation is employed here and the resulting set of equations are summarized in the Appendix. A list of the resulting model constants is given in Table 1.

Comparison with Vorticity Transport Theory

It is useful to contrast the present model with the vorticity transport model.[4–7] The present approach is based on the Boussinesq assumption and employs the enstrophy equation in place of ε or ω equations to effect closure. In the vorticity transport theory the turbulent stress in the momentum equation is eliminated using the identity indicated in Eq. (8), i.e.,

$$\frac{\partial}{\partial x_i}\overline{(u_m' u_i')} = \frac{\partial k}{\partial x_m} + \varepsilon_{mij}\overline{\omega_i' u_j'} \tag{31}$$

Instead of modeling the turbulent stress, attention is focused on modeling $\overline{\omega_i' u_j'}$. In this work, this quantity is modeled in Eq. (13), whereas in vorticity transport theory the term is modeled as[4–7]

$$\overline{\omega_i' u_j'} = -T\overline{u_j' u_k'}\frac{\partial \Omega_i}{\partial x_k} + Q\overline{u_j'\frac{\partial u_i'}{\partial x_k}}\Omega_k \tag{32}$$

where T and Q are Lagrangian integral scales and can depend on the indices employed. Thus, in the most general case, the number of T scales is 9 and the number of Q scales is 27. In addition, $\overline{u_i' \partial u_i'/\partial x_k}$ needs to be modeled.

Gorski[7] implemented a two-dimensional version of the preceding approach using a k-enstrophy model to effect closure. Because of the different nature of the two approaches, it is difficult to make a direct comparison between the enstrophy equation developed here and that of Ref. 7.

Results and Discussion

Because the k–ε model performs better than the k–ω for free shear flows,[1] comparisons with both experiment and the k–ε model are presented. As was pointed out by Paullay et al.,[12] solutions obtained using similarity equations have a high degree of accuracy and are well within 5% of solutions obtained from marching boundary-layer codes.

The first region considered is the self-similar region of the plane wake. Figure 1 compares computed mean velocity W, referred to its centerline value W_0, with experiment[13,14] and with the k–ε model. In cases where the data are not symmetric both sets of data are

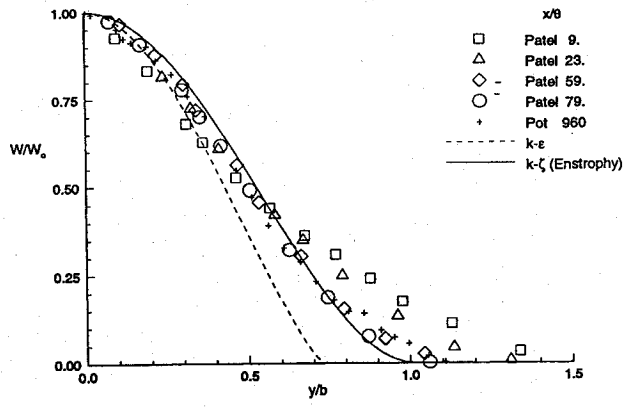

Fig. 1 Self-similar mean velocity, plane wake.

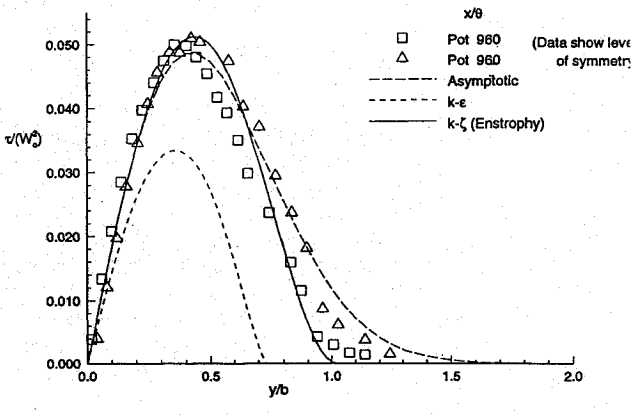

Fig. 2 Self-similar shear stress, plane wake.

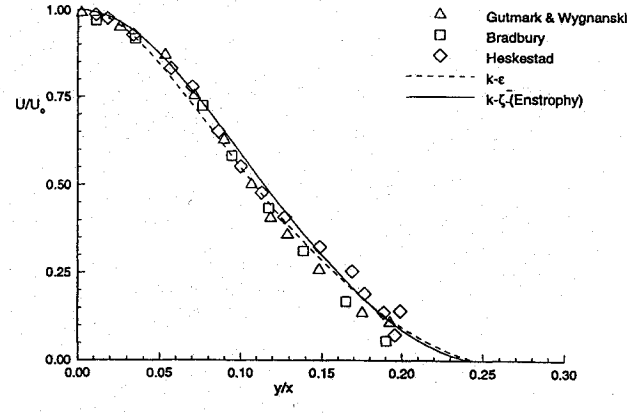

Fig. 3 Self-similar mean velocity, plane jet.

given. As is seen from the figure, computed profiles are in good agreement with experiment and show a noted improvement over the $k-\varepsilon$ model. Figure 2 shows similar comparisons for the shear stress. Included in the figure is a comparison with the asymptotic solution obtained by assuming ν_t to be constant. Again, marked improvement over the $k-\varepsilon$ model is seen, and good agreement with experiment is indicated. The b in Figs. 1 and 2 denotes half-width.

Figures 3 and 4 show comparisons with the mean velocity and shear stress for a two-dimensional jet. Both $k-\zeta$ and $k-\varepsilon$ models show good agreement with experiment.[15–17] Bradbury[16] indicates that his measured spreading rate is not exactly proportional to x. The departure from true self-preservation, however, is so small that no adjustment is necessary in Fig. 3. Figures 5 and 6 examine the round jet results. Here, the $k-\zeta$ model shows marked improvement over the $k-\varepsilon$ model and is in good agreement with experiment.[18,19] Figures 7 and 8 compare the $k-\zeta$ and $k-\varepsilon$ models for radial jets. Available data[20–22] suggest that profiles for the radial jet approach those for the plane jet. Since both turbulence models were in good agreement with experiment for the plane jet, the indicated agreement in Figs. 7 and 8 is expected.

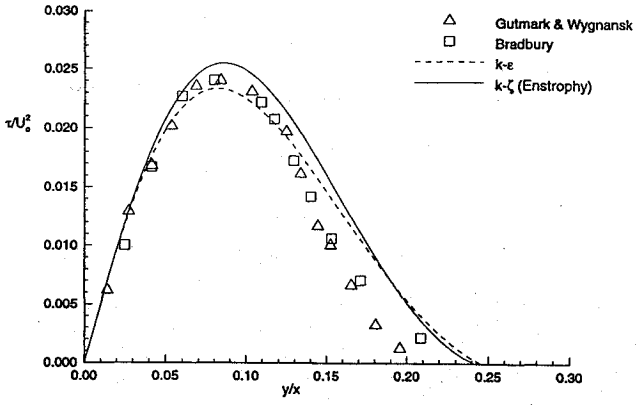

Fig. 4 Self-similar shear stress, plane jet.

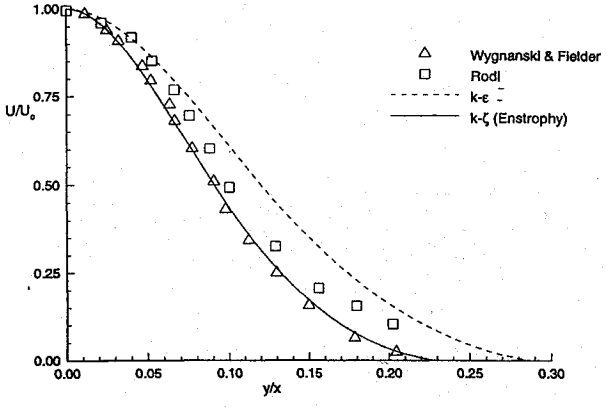

Fig. 5 Self-similar mean velocity, round jet.

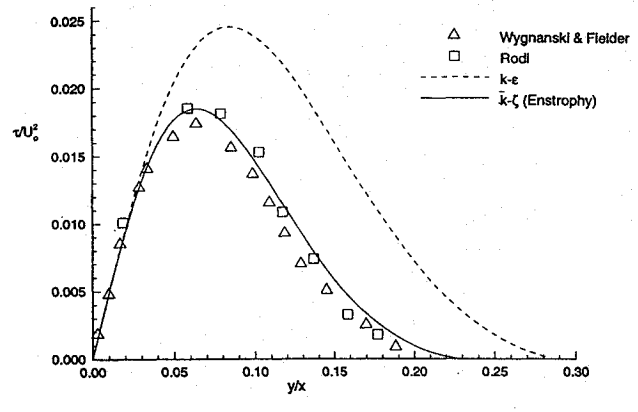

Fig. 6 Self-similar shear stress, round jet.

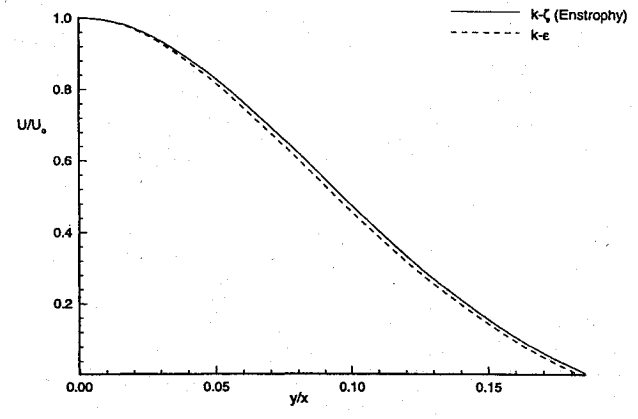

Fig. 7 Self-similar mean velocity, radial jet.

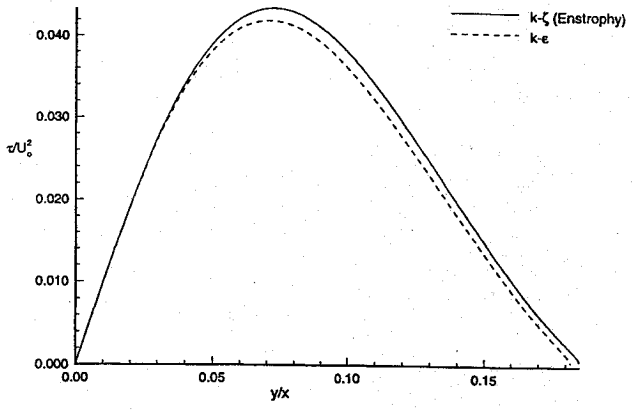

Fig. 8 Self-similar shear stress, radial jet.

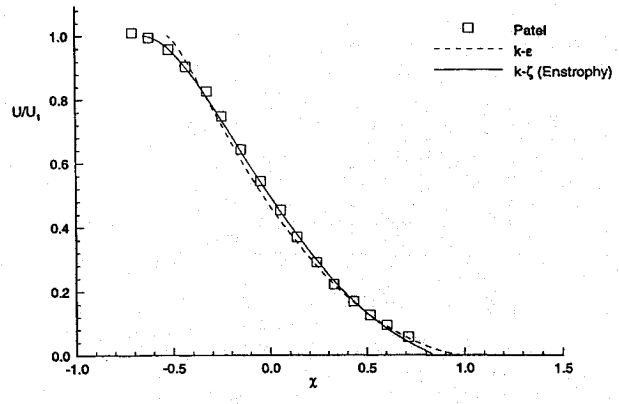

Fig. 9 Self-similar mean velocity, mixing layer.

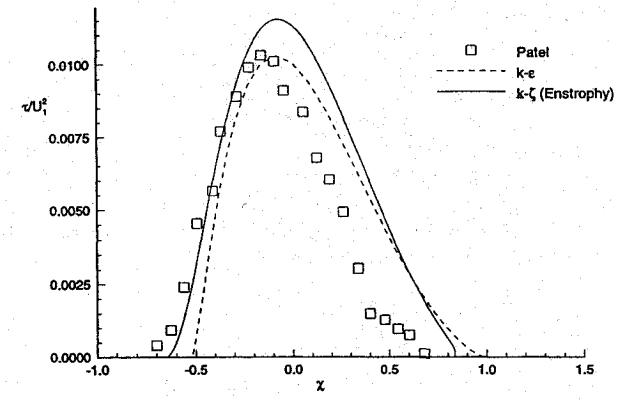

Fig. 10 Self-similar shear stress, mixing layer.

The final free shear flow considered is that of the mixing layer. In Figs. 9 and 10, U_1 is the freestream velocity, and χ is defined as

$$\chi = -\frac{(y/x) - (y/x)_{0.5}}{(y/x)_{0.9} - (y/x)_{0.1}} \tag{33}$$

where $(y/x)_{0.1}$, etc., denotes the location where the ratio of the mean velocity to that of the freestream is 0.1, etc. For this case, the mean velocity is accurately predicted. The theory shows good agreement with the predicted shear stress in the streaming side of the measurements but not with the zero velocity side. Patel[23] points out that measurements with a normal hot-wire probe became unreliable in the zero velocity side. However, no estimate of inaccuracies were given. Thus, a more accurate measurement in the zero velocity side is needed before a definitive statement can be made regarding predictions of the theory in this region.

A summary of calculated spreading rates is shown in Table 2. The spreading rates are defined in a manner consistent with that given in Table 2 of Ref. 1. In general, all growth rates calculated using the $k-\zeta$ model are well within experimental scatter. This may be contrasted with the $k-\varepsilon$ model especially for the plane wake and the round jet; for the former, the spreading rate is underpredicted by 30%, whereas for the latter, it is overpredicted by over 25–40%.

Table 2 Free shear flow spreading rates

Flow	$k-\zeta$	$k-\varepsilon$	Measured[1]
Far wake	0.3130	0.256	0.365
Mixing layer	0.1123	0.098	0.115
Plane jet	0.1145	0.109	0.100–0.110
Round jet	0.0906	0.120	0.086–0.096
Radial jet	0.0965	0.094	0.096–0.110

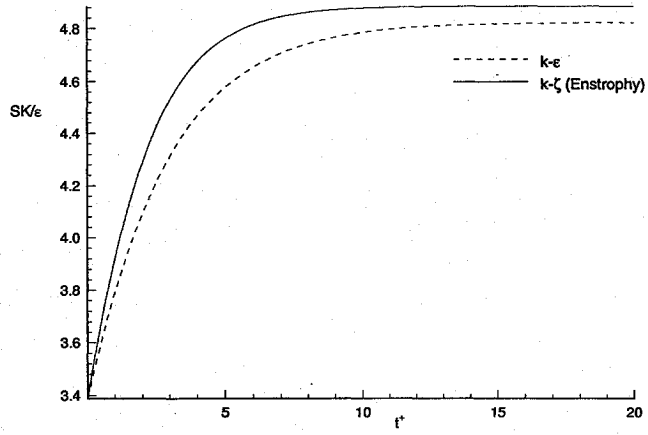

Fig. 11 Homogeneous shear parameter.

The final figure involves comparisons with the uniform shear flow. Measurements and direct numerical simulation[9] suggest that the shear parameter, SK/ε reaches an equilibrium value around 5. For uniform shear flows

$$S_{12} = S_{21} = S; \qquad S_{ij} = 0, \qquad \text{all others} \tag{34}$$

Figure 11 shows a comparison between $k-\zeta$ and $k-\varepsilon$ calculations. Although results of the decay of homogeneous turbulence were not involved in determining model constants in the present work, the present model gives a better prediction than the $k-\varepsilon$ model. Note that t^* in Fig. 11 is tS.

For decaying homogeneous isotropic turbulence, Eqs. (23) and (25) give

$$\frac{dk}{dt} = -\nu\zeta, \qquad \frac{d\zeta}{dt} = -\beta_5 \nu \frac{\zeta^2}{k} \tag{35}$$

Setting

$$\beta_5 = (m+1)/m = 2.37 \tag{36}$$

one concludes that the present model predicts a decay rate given by

$$k - t^{-m} = t^{-0.73} \tag{37}$$

This may be compared to values of m varying from 1 to 2.5 suggested for the decay of homogeneous turbulence. It may be also contrasted to a value of $m = 0.7$ suggested by Kolmogorov[24] and a value of $m = 0.844$ deduced by Dakos and Gibson[25] in their study of the decay of anisotropic homogeneous turbulence.

Concluding Remarks

The present model predicts the important features of all free shear flows using the same set of model conditions and boundary conditions. The success of the model is a result of the fact that the underlying equations are the exact equations that are valid for all turbulent Reynolds numbers and thus incorporate the correct physics. Moreover, it appears that the procedure used in modeling the various averages is appropriate.

Results obtained here seem to support the widely accepted notion that one of the primary reasons for the failure of existing turbulence models is a result of the inadequate modeling of the dissipation equation.

The model did not rely on the decay of homogeneous turbulence in determining model constants. When compared with the $k-\varepsilon$ model in describing homogeneous shear flows, however, it gave a better estimate of the value of the shear parameter at equilibrium. On the other hand, it produces a decay rate more representative of the decay of anisotropic homogeneous turbulence. The last result is somewhat unexpected and merits further examination.

Appendix: Similarity Form of Governing Equations

The similarity form of the governing equations can be obtained for the various free shear flows as follows.

Plane wake:

$$u(x,y) = U_\infty - \sqrt{\frac{\mathrm{D}}{\rho x}}G(\eta)$$

$$k(x,y) = \frac{\mathrm{D}}{\rho x}K(\eta) \qquad \zeta(x,y) = \frac{\mathrm{D}U_\infty E(\eta)}{\nu\rho x^2}$$

$$\nu_t = \frac{C_\mu K^2(\eta)}{E(\eta)}\left(\frac{\mathrm{D}}{\rho U_\infty}\right) \qquad N = C_\mu\frac{K^2(\eta)}{E(\eta)}$$

$$\eta = y\sqrt{\frac{\rho U_\infty^2}{\mathrm{D}x}}$$

Mixing layer:

$$u(x,y) = U_1 G(\eta) \qquad v(x,y) = U_1[V+\eta G]$$

$$k(x,y) = U_1^2 K(\eta) \qquad \zeta(x,y) = \left(U_1^3/\nu x\right)E(\eta)$$

$$\nu_t = \frac{C_\mu U_1 x K^2(\eta)}{E(\eta)} \qquad N = C_\mu\frac{K^2(\eta)}{E(\eta)} \qquad \eta = \frac{y}{x}$$

Jet (plane, round, and radial):

$$u(x,y) = U_0 G(\eta) \qquad v(x,y) = U_0 V(\eta)$$

$$G(\eta) = (\eta^m F)'/\eta^m \qquad V(\eta) = \eta G - 2^{j-1}F$$

$$k(x,y) = U_0^2 K(\eta) \qquad \zeta(x,y) = U_0^3 E(\eta)/\nu x$$

$$\nu_t = \frac{C_\mu K^2(\eta)U_0 x}{E(\eta)} \qquad N = C_\mu\frac{K^2(\eta)}{E(\eta)}$$

$$\eta = \frac{y}{x} \qquad U_0 = \frac{J}{x^{(j+1)/2}}$$

where $j = 0$ and $m = 0$ for planar jets; $j = 1$ and $m = 0$ for radial jets; and $j = 1$ and $m = 1$ for round jets; J is specific momentum flux.

Before solving the resulting ordinary differential equations the transformation introduced by Paullay et al.[12] is introduced. This transformation has the form

$$\frac{\mathrm{d}}{\mathrm{d}\xi} = N\frac{\mathrm{d}}{\mathrm{d}\eta} \tag{A1}$$

Using this substitution and the notation of Ref. 1, the momentum and turbulent kinetic energy equations take the form

$$\nu\frac{\mathrm{d}G}{\mathrm{d}\xi} - \frac{1}{\eta_j}\frac{\mathrm{d}}{\mathrm{d}\xi}\left(\eta_j\frac{\mathrm{d}G}{\mathrm{d}\xi}\right) = S_u NG \tag{A2}$$

$$\nu\frac{\mathrm{d}K}{\mathrm{d}\xi} - \frac{1}{\eta_j}\frac{\mathrm{d}}{\mathrm{d}\xi}\left(\frac{\eta_j}{\sigma_k}\frac{\mathrm{d}K}{\mathrm{d}\xi}\right) = S_k NK + \left(\frac{\mathrm{d}G}{\mathrm{d}\xi}\right)^2 - NE \tag{A3}$$

where ν, S_u, and S_k are given in Table 4.1 of Ref. 1.

The enstrophy equations for the plane wake, mixing layer, and the various jets are given as follows.

Plane wake:

$$\nu\frac{\mathrm{d}E}{\mathrm{d}\xi} - \frac{\mathrm{d}}{\mathrm{d}\xi}\left[\frac{1}{\sigma_\zeta}\frac{\mathrm{d}E}{\mathrm{d}\xi}\right] = 2EN - \beta_5\frac{E^2N}{K} + \frac{2}{3}\beta_4 E\left|\frac{\mathrm{d}G}{\mathrm{d}\xi}\right| + \frac{\alpha_3 C_\mu K}{N}\left(\frac{\mathrm{d}G}{\mathrm{d}\xi}\right)^2 + \frac{4}{3}\frac{\beta_6}{N}\left|\frac{\mathrm{d}G}{\mathrm{d}\xi}\right|^3 \tag{A4}$$

Mixing layer:

$$\nu\frac{\mathrm{d}E}{\mathrm{d}\xi} - \frac{\mathrm{d}}{\mathrm{d}\xi}\left[\frac{1}{\sigma_\zeta}\frac{\mathrm{d}E}{\mathrm{d}\xi}\right] = GEN - \beta_5\frac{E^2N}{K} + \alpha_3\frac{C_\mu K}{N}\left(\frac{\mathrm{d}G}{\mathrm{d}\xi}\right)^2 + \frac{2}{3}\beta_4 E\left|\frac{\mathrm{d}G}{\mathrm{d}\xi}\right| + \frac{4}{3}\left(\beta_8\Big/\frac{\mathrm{d}G}{\mathrm{d}\xi}\right)\frac{\mathrm{d}K}{\mathrm{d}\eta}NE + \frac{4}{3}\frac{\beta_6}{N}\left|\frac{\mathrm{d}G}{\mathrm{d}\xi}\right|^3 \tag{A5}$$

Jets (plane, round, and radial):

$$\nu\frac{\mathrm{d}E}{\mathrm{d}\xi} - \frac{1}{\eta^m}\frac{\mathrm{d}}{\mathrm{d}\xi}\left[\eta^m\frac{1}{\sigma_\zeta}\frac{\mathrm{d}E}{\mathrm{d}\xi}\right] = GEN[1+3(2^{j-1})] + \frac{\alpha_3 E}{K}\left[\left(\frac{\mathrm{d}G}{\mathrm{d}\xi}\right)^2 + 2N^2 j\left(\frac{\eta G+\nu}{\eta^j}\right)^2\right] + \beta_5\frac{NE^2}{K} - \beta_4 E\left|\frac{\mathrm{d}G}{\mathrm{d}\xi}\right|\left[\frac{2Nj}{\eta^j K}(\eta G+\nu) - \frac{2}{3}\right] - \beta_6\left|\frac{\mathrm{d}G}{\mathrm{d}\xi}\right|^3\left[\frac{4Nj}{\eta^j K}(\eta G+\nu) - \frac{4}{3N}\right]\frac{\beta_7 ENj}{\eta^j}(\eta G+\nu) + \left(\beta_8 N\Big/\frac{\mathrm{d}G}{\mathrm{d}\xi}\right)\left(\frac{4Nj}{\eta^j K}(\eta G+\nu) - \frac{4}{3}\right) \times\left[2^j K\frac{\mathrm{d}E}{\mathrm{d}\xi} - 3E\frac{\mathrm{d}K}{\mathrm{d}\xi}2^{j-1} - E\frac{\mathrm{d}K}{\mathrm{d}\xi}\right]$$

Acknowledgments

This work is supported in part by the following grants: NASA Grant NAG-1-244 and the Mars Mission Research Center funded by NASA Grant NAGW-1331. The authors would like acknowledge many helpful discussions with E. C. Anderson, Senior Research Scientist at the NASA Langley Research Center.

References

[1]Wilcox, D. C., "Turbulence Modeling for CFD," DCW Industries, Inc., La Cañada, CA, 1993.

[2]Morse, A. P., "Axisymmetric Free Shear Flows With and Without Swirl," Ph.D. Dissertation, Imperial College of Science and Technology, Univ. of London, London, May 1980.

[3]Tennekes, H., and Lumley, J. L., *A First Course in Turbulence*, MIT Press, Cambridge, MA, 1989, p. 87.

[4]Bernard, P. S., and Berger, B. S., "A Method for Computing Three-Dimensional Turbulent Flows," *Journal of Applied Mathematics*, Vol. 43, No. 3, 1982, pp. 453–470.

[5]Raul, R., and Bernard, P. S., "A Numerical Investigation of the Turbulent Flow Field Generated by a Stationary Cube," *Journal of Fluids Engineering*, Vol. 113, June 1991, pp. 216–222.

[6]Bernard, P. S., "Turbulent Vorticity Transport in Three Dimensions," *Theoretical and Computational Fluid Dynamics*, Vol. 2, No. 1, 1990, pp. 165–183.

[7]Gorski, J. J., "Application of Vorticity Transport Analysis to the Development of Physically Accurate Turbulence Models," Ph.D. Dissertation, Univ. of Maryland, College Park, MD, 1993.

[8]Reynolds, W. C., "Fundamentals of Turbulence for Turbulence Modeling and Simulation," AGARD R-755, Special Course on Modern Theoretical and Experimental Approaches to Turbulent Flow Structure and its Modeling, 1987, pp. 1.1–1.66.

[9]Bernard, P. S., and Speziale, C. G., "Bounded Energy States in Homogeneous Turbulent Shear Flows—An Alternative View," *Journal of Fluids Engineering*, Vol. 114, No. 1, 1992, pp. 29–39.

[10]Pope, S. B., "An Explanation of the Turbulent Round-Jet/Plane-Jet Anomaly," *AIAA Journal*, Vol. 16, No. 3, 1978, pp. 279–281.

[11]Rubel, A., "On the Vortex Stretching Modification of the $k-\varepsilon$ Turbulence Model: Radial Jets," *AIAA Journal*, Vol. 23, No. 7, 1985, pp. 1129, 1130.

[12]Paullay, A. J., Melnik, R. E., Rubel, A., Rudman, S., and Siclari, M. J., "Similarity Solutions for Plane and Radial Jets Using $k-\varepsilon$ Turbulence Model," *Journal of Fluids Engineering*, Vol. 107, March 1985, pp. 79–85.

[13]Ramaprian, B. R., Patel, V. C., and Sastry, M. S., "The Symmetric Turbulent Wake of a Flat Plate," *AIAA Journal*, Vol. 20, No. 9, 1982, pp. 1228–1235.

[14]Pot, P. J., "Measurement in a Two-Dimensional Wake and in a Two-Dimensional Wake Merging into a Boundary Layer," National Aerospace Lab., Data Rept. NLR TR-79063 U, The Netherlands, 1979.

[15]Gutmark, E., and Wygananski, I., "The Planar Turbulent Jet," *Journal of Fluid Mechanics*, Vol. 73, Pt. 3, 1976, pp. 465–495.

[16]Bradbury, L. J., "The Structure of the Self-Preserving Jet," *Journal of Fluid Mechanics*, Vol. 23, Pt. 1, 1965, pp. 31–64.

[17]Heskestad, G., "Hot-Wire Measurements in a Plane Turbulent Jet," *Journal of Applied Mechanics*, Vol. 32, No. 4, 1965, pp. 721–734.

[18]Wygnanski, I., and Fiedler, H. E., "The Two-Dimensional Mixing Region," *Journal of Fluid Mechanics*, Vol. 41, Pt. 2, 1970, pp. 327–361.

[19]Rodi, W., "A New Method of Analyzing Hot-Wire Signals in Highly Turbulent Flows and Its Evaluation in Round Jets," Disa Information, No. 17, 1975.

[20]Heskestad, G., "Hot-Wire Measurements in a Radial Turbulent Jet," *Journal of Applied Mechanics*, Vol. 33, No. 2, 1966, pp. 417–424.

[21]Tanaka, T., and Tanaka, E., "Experimental Study of a Radial Turbulent Jet," *Bulletin of the Japan Society of Mechanical Engineers*, Vol. 19, No. 133, 1976, pp. 792–799.

[22]Witze, P. O., and Dwyer, H. A., "The Turbulent Radial Jet," *Journal of Fluid Mechanics*, Vol. 75, Pt. 3, 1976, pp. 401–417.

[23]Patel, R. P., "An Experimental Study of a Plane Mixing-Layer," *AIAA Journal*, Vol. 11, No. 1, 1973, pp. 67–71.

[24]Kolmogorov, A. N., "Equations of Turbulent Motion in Incompressible Fluid," *Izvestiya, Academy of Sciences, USSR, Physics (Atmospheric and Oceanic), Izvestiya Akademii Nauk SSSR*, Vol. 6, Nos. 1 and 2, 1994, pp. 56–58.

[25]Dakos, T., and Gibson, M. M., "The Decay of Anisotropic Homogeneous Turbulence," *Engineering Turbulence: Modeling and Experiments*, edited by W. Rodi and E. N. Ganic, Elsevier, New York, 1990, pp. 73–82.